Journal of Neurochemistry

JOURNAL OF NEUROCHEMISTRY | 2010 | 114 | 832–842

doi: 10.1111/j.1471-4159.2010.06811.x

Neurite-like structures induced by mevalonate pathway blockade are due to the stability of cell adhesion foci and are enhanced by the presence of APP

Mary Hughes,* Vladimir Snetkov,† Ruth-Sarah Rose,* Sebastian Trousil,* Jacqueline E. Mermoud‡ and Colin Dingwall*

*Pharmaceutical Sciences Division and †Asthma, Allergy and Lung Biology Division, King's College London, London, UK

‡Chromatin and Gene Expression Laboratory, The Babraham Institute, Babraham, Cambridge, UK

Abstract

Epidemiological studies have shown an association between statin use and a decreased risk of dementia. However, the mechanism by which this beneficial effect is brought about is unclear. In the context of Alzheimer's disease, at least three possibilities have been studied; reduction in amyloid β peptide (Aβ) production, the promotion of α-secretase cleavage and positive effects on neurite outgrowth. By investigating the effects of mevalonate pathway blockade on neurite outgrowth using real-time imaging, we found that rather than promote the production of neurite extensions, inhibition rapidly induced cell rounding. Crucially, neurite-like structures were generated through the persistence of cell–cell and cell–substrate adhesions and not through a mechanism of positive outgrowth. This effect can be strikingly enhanced by the over-expression of human amyloid precursor protein and is isoprenoid rather than cholesterol dependent.

Keywords: adhesion, amyloid precursor protein, cerulenin, mevalonate, statins.

J. Neurochem. (2010) **114**, 832–842.

The statins are the major cholesterol lowering agents in the clinic for patients at risk of cardiovascular disease. Epidemiological studies have established a link between the use of statins and a lowered risk of developing Alzheimer's disease (AD) (Jick *et al.* 2000; Wolozin *et al.* 2000; Zamrini *et al.* 2004; Fonseca *et al.* 2009). AD is the predominant form of dementia in the elderly and consequently these studies have stimulated research into how statins affect cellular mechanisms relevant to AD. While it is unclear exactly how statin treatment leads to a reduction in risk, there is significant evidence to suggest that statins affect amyloid precursor protein (APP) processing and can have profound effects on cell and neurite morphology.

The neurotoxic amyloid β peptide (Aβ) initiates a pathological cascade leading to synaptic and neuron loss in AD (Walsh *et al.* 2000). Aβ is generated through sequential cleavage of APP by beta site APP cleaving enzyme 1 (BACE1) and the γ-secretase complex and is thought to occur predominantly in endosomes (Kinoshita *et al.* 2003; Rajendran *et al.* 2006; Small and Gandy 2006). APP and BACE1 co-localise in cholesterol-rich microdomains or 'lipid rafts', and β-cleavage is thought to be enhanced in these domains (Riddell *et al.* 2001; Cordy *et al.* 2003). Statins have been demonstrated to reduce the production of Aβ in at least two systems; in the CNS in animal models of AD and in cell based assays (Fassbender *et al.* 2001; Hoglund and Blennow 2007). The lowering of Aβ production is a result of a reduction in APP trafficking to lipid rafts and inhibition of APP trafficking to the endocytic pathway (Simons *et al.* 1998; Fassbender *et al.* 2001; Kojro *et al.* 2001; Ehehalt *et al.* 2003; Won *et al.* 2008).

Although the β secretase pathway is important in AD pathogenesis, quantitatively the majority of APP is cleaved

Received November 5, 2009; revised manuscript received April 15, 2010; accepted May 5, 2010.

Address correspondence and reprint requests to Colin Dingwall, Pharmaceutical Sciences Division, King's College London, Franklin-Wilkins Building, 150 Stamford Street, London SE1 9NH, UK.
E-mail: colin.dingwall@kcl.ac.uk

Abbreviations used: AD, Alzheimer's disease; ADAM, a disintegrin and metalloprotease; APP, amyloid precursor protein; Aβ, amyloid β peptide; BACE1, beta site APP cleaving enzyme 1; CL, cerulenin; DMEM, Dulbecco's modified Eagle's medium; FPP, farnesyl pyrophosphate; GGPP, geranylgeranyl pyrophosphate; HMG-CoA, 3-hydroxy-3-methyl glutaryl CoA; PARP, anti-poly (ADP-ribose) polymerase.

by α-secretase pathway. Several members of the ADAM (a disintegrin and metalloprotease) family of metalloproteases show α-secretase activity and cleave APP within the Aβ domain, precluding Aβ generation. Inhibition of APP trafficking to endosomes by statins favours α-cleavage which occurs predominantly at the plasma membrane (Sisodia 1992). Statins also cause up-regulation of the expression of the α-secretase ADAM 10, which further promotes non-amyloidgenic APP cleavage (Kojro *et al.* 2001).

Statins inhibit 3-hydroxy-3-methyl glutaryl CoA (HMG-CoA) reductase which catalyses the rate limiting step in cholesterol and isoprenoid biosynthesis. Initially, it was thought that the cholesterol lowering effect of statins was directly responsible for the effect on APP processing through disrupting lipid rafts since the effects of statins could be reversed by cholesterol addition (Simons *et al.* 1998; Parsons *et al.* 2007). However, a growing body of data indicates that isoprenoid depletion is the key factor. Concentrations of statins which do not alter the cholesterol content of lipid rafts, can nevertheless prevent APP localisation within these membrane domains and thus APP processing (Won *et al.* 2008). In the AD brain, cholesterol levels are maintained but isoprenoid homeostasis is dysregulated (Eckert *et al.* 2009). Increasing evidence demonstrates the importance of isoprenoids in the modulation of APP processing (Cole and Vassar 2006). The covalent attachment of isoprenoids to proteins is important in regulating the membrane association of members of the GTPase superfamily (Resh 2006). Members of the Rab and Rho GTPase families regulate vesicle trafficking and the activity of these proteins is reduced by statin treatment which directly influences APP localisation and processing (McConlogue *et al.* 1996; Kroschewski *et al.* 1999; Ehehalt *et al.* 2003; Maillet *et al.* 2003; Pedrini *et al.* 2005; Ostrowski *et al.* 2007; Won *et al.* 2008).

In addition to the effects on APP processing, the treatment of cells in culture with statins induces a number of striking morphological changes, but the published reports differ significantly. For example, statin treatment of primary neurons has been reported to cause process retraction (Meske *et al.* 2003; Kim *et al.* 2009). However, other studies report the positive promotion of neurite outgrowth (Pooler *et al.* 2006). In neuronal cell lines, further ambiguity exists. Statins have been suggested to cause isoprenoid dependent differentiation with accompanying neurite outgrowth (Maltese and Sheridan 1985; Fernandez-Hernando *et al.* 2005), but in other studies neurite retraction and cell rounding are observed (Schmidt *et al.* 1982; Koch *et al.* 1997; Agarwal *et al.* 2002; Schulz *et al.* 2004). One consistent feature in these studies is that isoprenoid rather than cholesterol depletion is linked to morphological change.

To begin to resolve the controversy surrounding the morphological effects induced by inhibition of isoprenoid and cholesterol synthesis, we focussed on the dynamics of the changes in cell morphology using video microscopy. We have used two representative and specific inhibitors of isoprenoid and cholesterol synthesis. Simvastatin is a reversible inhibitor of the rate limiting enzyme of mevalonate synthesis HMG-CoA reductase (EC 1.1.1.88) (Alberts 1990). Cerulenin is an inhibitor of HMG-CoA synthase (EC 2.3.3.10) (Omura 1976; Malvoisin and Wild 1990). Both of these enzymes are subject to up-regulation by cholesterol-mediated feedback (Brown and Goldstein 2009). Our live-cell imaging analysis revealed that treatment of cells with either simvastatin or cerulenin results in contraction of the cell body. Neurite-like structures or 'tails' are formed as observed previously, but our key observation is that they arise, not from positive outgrowth but from the persistence of cell–cell and cell-to-substrate adhesion as the cell rounds. We discovered that APP plays an important role in this process, as its over-expression markedly enhanced the persistence of cell–cell and cell-to-substrate adhesion but did not affect cell rounding.

Materials and methods

Reagents

Anti-poly (ADP-ribose) polymerase (PARP) antibodies were obtained from Cell Signalling Technology (Hertfordshire, UK). Beta secretase inhibitor IV was purchased from Calbiochem (Darmstadt, Germany). ADAM 10 pro-domain was from Biozyme Incorporated (Apex, NC, USA).

All other reagents were purchased from Sigma-Aldrich chemical company (Poole, UK) unless otherwise stated in the text.

Cell culture

SH-SY5Y ($5Y^0$) cells were maintained in Dulbecco's modified Eagle' medium (DMEM) supplemented with 2 mM glutamine and 10% v/v foetal bovine serum. Stable cell lines over-expressing APP containing the Swedish mutation $APP_{K595N,\ M596L}$ (APP_{swe}) (Hussain *et al.* 2007) or the empty vector PcDNA3.1 (Invitrogen, Carlsbad, CA, USA) ($5Y_{PcDNA3.1}$) were further supplemented with 0.5 mg/mL geneticin. Cerulenin (CL) was dissolved to 10 mg/mL in absolute EtOH. Simvastatin was dissolved to 10 mM in dimethylsulfoxide. Cholesterol, complexed with cyclodextrin (Sigma) was dissolved in water. A soluble 10 mM solution of palmitate was made as described in (Pimenta *et al.* 2008). Briefly, sodium palmitate was dissolved in absolute EtOH and complexed with fatty acid-free albumin in a 12.5% w/v solution in Optimem (Invitrogen, Carlsbad, CA, USA). Farnesyl pyrophosphate (FPP) and geranylgeranyl pyrophosphate (GGPP) were obtained as 1 mg/mL solutions in MeOH : NH_4OH (7 : 3) from Sigma. Solutions were diluted 1 : 1 in 12.5% fatty acid-free albumin solution and further diluted in Optimem for addition to cells. Cells were pre-treated with compound (palmitate, cholesterol, FPP, geranygeranyl pyrophosphate, α, β, γ-secretase inhibitors or Y27632) for 3 h prior to the addition of CL. The final concentrations used are indicated in the text.

All controls contained an equivalent concentration of the corresponding solvent.

Imaging and video microscopy

Phase contrast images were taken using a Nikon eclipse TE 2000-S (Nikon Instruments Europe B.V, Kingston, Surrey, UK) with a 20× objective. Images were processed using NIS elements F version 2.20 (Nikon).

For video microscopy cells were seeded on a cover slip housed in a chamber maintained at 37°C in Kreb's solution equilibrated with air/5% CO_2 (NaCl 118 mM, $NaHCO_3$ 24 mM, KCl 4 mM, $CaCl_2$ 1.8 mM, $MgSO_4$ 1 mM, NaH_2PO_4 0.43 mM, Glucose 5.6 mM). Images were taken using a Zeiss Axiovert 200 (Carl Zeiss Ltd, Welwyn Garden City, Hertfordshire, UK) with a long distance 40× phase contrast objective, with Metamorph Software v. 6 (Molecular Devices, Sunnyvale, CA, USA). Images were acquired every 30 s for 2–3 h. Videos are played at a speed of 15 frames per second (Videos S1–S5).

Quantification of morphological differentiation

Processes are defined as structures having a length greater than the diameter of the cell. We noted a slight positive correlation between the cell density and the number of processes observed (Figure S1). On the basis of this data, we ensured equal cell plating density in all experiments. The *n* values given in the text and figures are number of experimental repeats. In each repeat experiment, two fields of view were selected at random, each containing at least 50 cells, and the number of processes per cell was counted. Hence, at least 100 cells were counted in each experiment. Where a process from one cell fused to a neighbouring cell, the process was counted once. Cells which had begun to contract were clearly distinguished by having a rounded, symmetrical, phase bright appearance as opposed to a flat polygonal morphology. The percentage of rounded cells was also counted per treatment. Branches were defined as structures that originated from, and were at least the width of, the processes.

Cell adhesion assay

Cells were harvested using Cell Dissociation Solution (Sigma) and seeded at 2.5×10^4 cells per well in a 96-well plate in DMEM. At each time point, the medium was removed and the wells were washed thrice with phosphate-buffered saline to remove non-adhered cells and the cells were supplemented with fresh DMEM. After the washing steps, the remaining adhered cells were lysed using Complete lysis buffer (Roche, Indianapolis, IN, USA) and the protein concentration was quantified as above. The protein concentration of the adhered cells at each time point was expressed as a proportion of the total seeded protein (cells). Protein concentration rather than cell number was measured as this allowed the rapid analysis of a large number of samples.

Statistical analysis

At least three independent experiments were performed for each condition. Statistical analyses were made using the SigmaStat software package (Systat Software Inc., San Jose, CA, USA). Student's *t*-test, one and two-way ANOVAS were conducted as indicated in the text, followed by a Tukey's test to assess significant interactions. A p value of < 0.05 was considered significant.

Results

Mevalonate pathway blockade induces profound morphological changes in neuroblastoma cells

To investigate the effects of inhibition of isoprenoid and cholesterol biosynthesis on cell morphology, we selected Simvastatin, an inhibitor of HMG-CoA reductase and CL, an inhibitor of HMG-CoA synthase (Fig. 1a). Untreated, non-transfected SH-SY5Y cells ($5Y^0$) grow as clusters of neuroblastic cells with multiple, short, fine cell processes (Fig. 1b). Over-expression of human APP carrying the Swedish mutation; K595N, M596L, 695 isoform numbering (APP_{swe}) did not alter this morphology (Fig. 1b). Consistent with previous reports, we found that treatment of human $5Y^0$ cells with Simvastatin (referred to from now in as statin) or CL induced the appearance of characteristic long processes and rounded cell bodies (Fig. 1c and d). However, we observed two striking differences between the effects of statin and CL treatments on the generation of these processes. First, statin treatment induces the generation of processes in SH-SY5Y cells independently of whether they over-express human APP (Fig. 1c). In contrast, the response to CL differs between the APP_{swe} cell line and non-transfected cells ($5Y^0$) such that APP markedly enhances the formation of processes (Fig. 1d). Second, the time taken for processes to appear differs; processes are evident within 3 h of CL treatment while processes are not apparent until 18–24 h of statin treatment.

To obtain a quantitative measure of these changes, we determined the average number of processes per cell, a process being defined as a structure having a length greater than the diameter of the cell, and the proportion of rounded cells (see Materials and methods). With statin treatment, we found no significant differences in the number of processes formed in $5Y^0$ and APP_{swe} cells (Fig. 1). In contrast, APP_{swe} cells developed strikingly more processes following CL treatment than $5Y^0$ cells (Fig. 1e). We found no difference in the proportion of rounded cells between $5Y^0$ and APP_{swe} (Fig. 1f). We have eliminated possible effects of selection by geneticin or the DNA vector by comparing the response of APP_{swe} with the geneticin-resistant cell line transfected with the empty vector (Fig. 1).

Cerulenin-induced changes are independent of secretase activity and *de novo* protein synthesis

We chose to investigate the effect of CL in more detail as treatment with this compound gave striking differential effects on process generation depending upon the over-expression of APP. We considered that these differences to be consistent with published reports that APP promotes cell adhesion to the extracellular matrix and between cells and our own observations that APP_{swe} cells are more adherent than $5Y^0$ cells (Fig. S2; Qiu *et al.* 1995; Soba *et al.* 2005). In addition to the role of full-length APP in cell adhesion, the

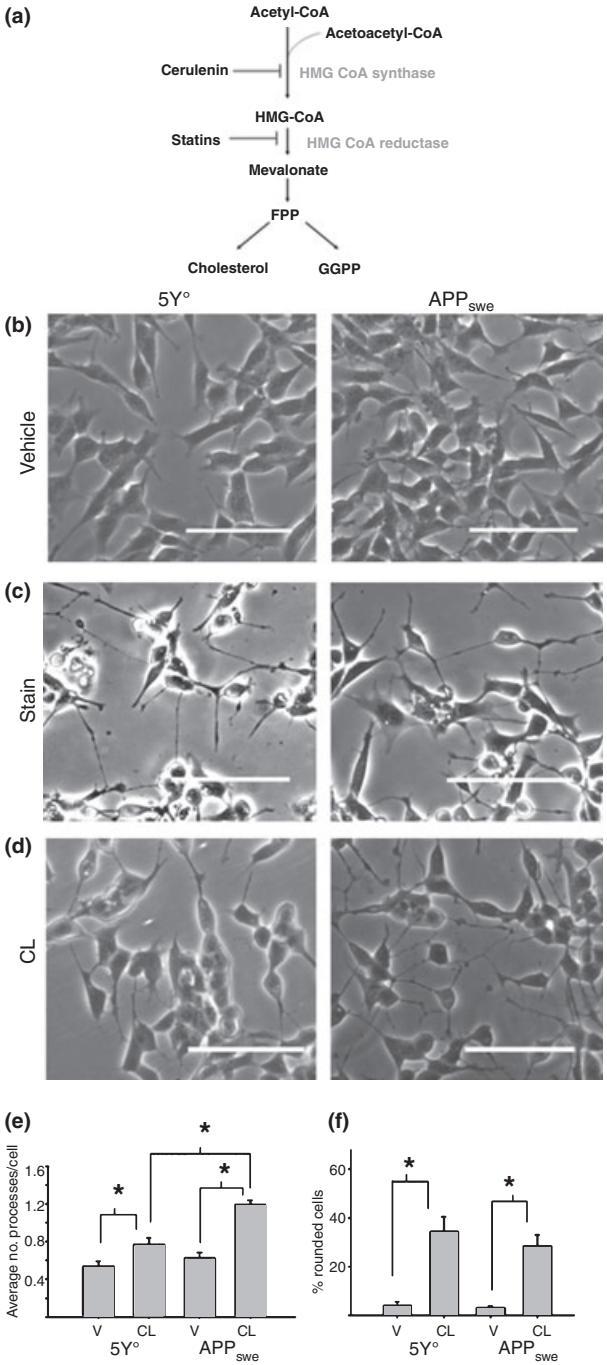

Fig. 1 Morphological change in response inhibition of mevalonate synthesis by cerulenin (CL) and Simvastatin. (a) The mevalonate biosynthetic pathway showing points of inhibition by statins and CL. (b) $5Y^0$ cells (left panel) and Swedish mutation amyloid precursor protein$_{K595N,\ M596L}$ (APP_{swe}) cells (right panel) following treatment with vehicle. (c) $5Y^0$ cells (left panel) and APP_{swe} cells (right panel) following 24 h treatment with 10 μM Simvastatin (statin). (d) $5Y^0$ cells (left panel) and APP_{swe} cells (right panel) following treatment with 100 μM CL for 3 h. (e) Average number of processes observed in $5Y^0$ cells and APP_{swe} cells following treatment with 100 μM CL for 3 h. Two-way ANOVA, $p < 0.05$, $n = 14$. (f) Percentage of rounded cells observed in $5Y^0$ cells and APP_{swe} cells following treatment with 100 μM CL for 3 h. Two-way ANOVA, $p < 0.05$, $n = 14$. Average number of processes per cell following Simvastatin treatments, $5Y^0 = 0.87 \pm 0.15$, $APP_{swe} = 0.97 \pm 0.06$. Average number of processes per cell in $5Y_{PcDNA3.1}$ following CL treatment compared with APP_{swe} cells: $5Y_{PcDNA3.1}$ Vehicle = 0.62 ± 0.1, $5Y_{PcDNA3.1}$ CL = 0.75 ± 0.04, APP_{swe} Vehicle = 0.61 ± 0.06, APP_{swe} CL = 1.09 ± 0.07. Two-way ANOVA, $p < 0.05$, $n = 3$. While we did not undertake a detailed quantitative analysis, the processes tended to be longer in Simvastatin than CL-treated cells. With 24 h treatment, cells receiving simvastatin began to fragment but remained attached to the wells, cells treated with CL completely rounded, the processes were retracted and the cells detached from the wells. Scale bars represent 100 μm.

cleaved soluble ectodomain has been demonstrated to have trophic activity (Araki *et al.* 1991; Ohsawa *et al.* 1995) and promote neurite outgrowth (Clarris *et al.* 1994; Jin *et al.* 1994) (Golde and Younkin 2001). Therefore, to determine whether APP cleavage was required for the changes we have observed, APP_{swe} were pre-treated with well characterised, potent and selective α, β, and γ, secretase inhibitors prior to the addition of CL. ADAM 10 pro-domain peptide, BACE1 inhibitor IV and *N*-[*N*-(3,5-difluorophenacetyl)-L-alanyl]-*S*-phenylglycine-*t*-butyl ester were used to inhibit α-, β- and γ- secretases, respectively (Morohashi *et al.* 2006; Moss *et al.* 2007; Itoh *et al.* 2009). None of these inhibitors modulated the effects of CL with respect to process generation, demonstrating that APP cleavage was not required for the increased number of processes in APP_{swe} cells compared with $5Y^0$ cells (Fig. 2a and Table S1).

Previous studies have suggested that statin-mediated morphological changes require protein synthesis in some cases (Koch *et al.* 1997) but not in others (Maltese and Sheridan 1985). To determine whether the observed morphological changes induced by CL treatment are similarly dependent upon *de novo* protein synthesis, we pre-treated APP_{swe} cells with cyclohexamide prior to the addition of CL and saw no difference in the observed morphology, indicating that protein synthesis is not required for this effect (Fig. 2b). CL has been reported to be an irreversible inhibitor (Price *et al.* 2001), which is consistent with our observation that CL-induced morphological change could not be reversed by incubating cells in CL-free medium after CL treatment (data not shown). CL, and the statins, has been shown to induce apoptosis after long-term exposure (Chung *et al.* 2006). Importantly, at the time points analysed here, rounding of cells and the appearance of processes in APP_{swe} cells was not accompanied by caspase cleavage of PARP, an early indicator of apoptosis, using staurosporine-induced PARP cleavage as a control. Using an antibody that preferentially recognises cleaved PARP, we detected minimal cleavage in CL-treated APP_{swe} cells, even after 6 h of treatment (Fig. 2c). Furthermore, we observed no apoptosis-related changes in nuclear morphology in cells treated with CL for 3 h and stained with 4′,6-diamidino-2-

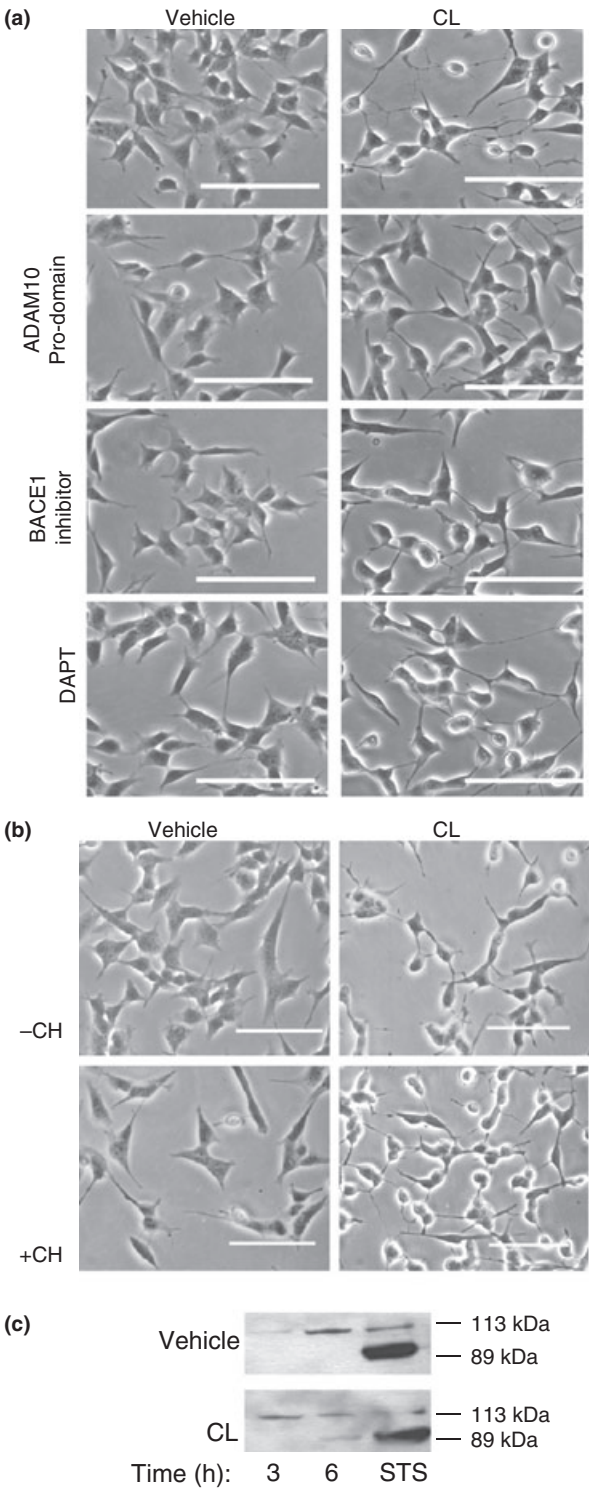

Fig. 2 Morphological change induced by cerulenin (CL) is independent of amyloid precursor protein (APP) cleavage and *de novo* protein synthesis. (a) Swedish mutation $APP_{K595N, M596L}$ (APP_{swe}) cells were treated with 2 μM ADAM (a disintegrin and metalloprotease) 10 prodomain, 5 μM beta site APP cleaving enzyme 1 (BACE1) inhibitor IV or 20 μM DAPT for 3 h prior to the addition of CL (100 μM) and incubation for a further 3 h. (b) AAP_{swe} cells were pre-treated with 5 μM cycloheximide for 1 h prior to the addition of CL (100 μM) and incubation for a further 3 h. Scale bars represent 100 μm. (c) Immunoblot showing lack of anti-poly (ADP-ribose) polymerase (PARP) cleavage in APP_{swe} cells after treatment with CL (100 μM) for 3 and 6 h; vehicle (upper gel); CL (lower gel). Staurosporine: PARP cleavage induced by incubation of cells with Staurosporine (1 μM for 6 h). Top band is uncleaved PARP. Arrow indicates cleaved PARP band.

phenylindole (data not shown). In conclusion, the changes observed are not simply a consequence of cell death.

SH-SY5Y cells can be differentiated using retinoic acid or growth factor stimulation (Simpson *et al.*, 2001, Monaghan *et al.*, 2007, Constaninescu *et al.*, 2007, Guarnieri *et al.*, 2009). This occurs over a period of several days and coincides with the appearance of several differentiation specific markers. This contrasts with the rapid effects of statin and CL we have observed. To eliminate the possibility that these treatments induce differentiation, we have carried out RT-PCR analysis for β-III tubulin and growth associated protein 43, two differentiation makers upon CL treatment and found no change in these markers (Fig. S3).

Cerulenin-induced changes are isoprenoid dependent

In addition to inhibiting the mevalonate pathway, CL also inhibits β-ketoacyl synthase (EC 2.3.1.41) (Fig. 3a), which results in lowered levels of palmitic acid (Omura 1976; Funabashi *et al.* 1989; Haapalainen *et al.* 2006). To determine which product of these pathways is involved in the observed effects, cells were treated with palmitate, cholesterol, or the isoprenoids FPP or GGPP for 3 h prior to CL treatment. Neither palmitate nor cholesterol affected the CL-induced morphological change at concentrations up to 100 μM (Fig. 3d). However, the addition of GGPP had a dramatic effect and FPP a modest effect in preventing the morphological change induced by CL in terms of the number of processes per cell (Fig. 3b,d). We obtained further evidence that the CL-induced morphological change is independent of fatty acid synthesis. Using tetradecyloxy-2 furoic acid, a specific inhibitor of acetyl-CoA carboxylase which lowers palmitate availability tetradecyloxy-2 furoic acid (Pizer *et al.* 2000), we observed no change in cell morphology compared with controls (Fig. 3c and Table S1).

Live-cell imaging reveals that processes are not generated by positive outgrowth

To reveal exactly how processes are generated by statin or CL treatment, we used time-lapse video microscopy. In the absence of any treatment APP_{swe} cells generated 2–3 short, highly motile protrusions per cell (Fig. 4 and Video S1). Cells interacted via short broad protrusions forming cell-to-cell contacts. As the cells separated, a short process-like bridge was formed between the cells. Process-like structures were also formed at the rear of migrating cells and have been

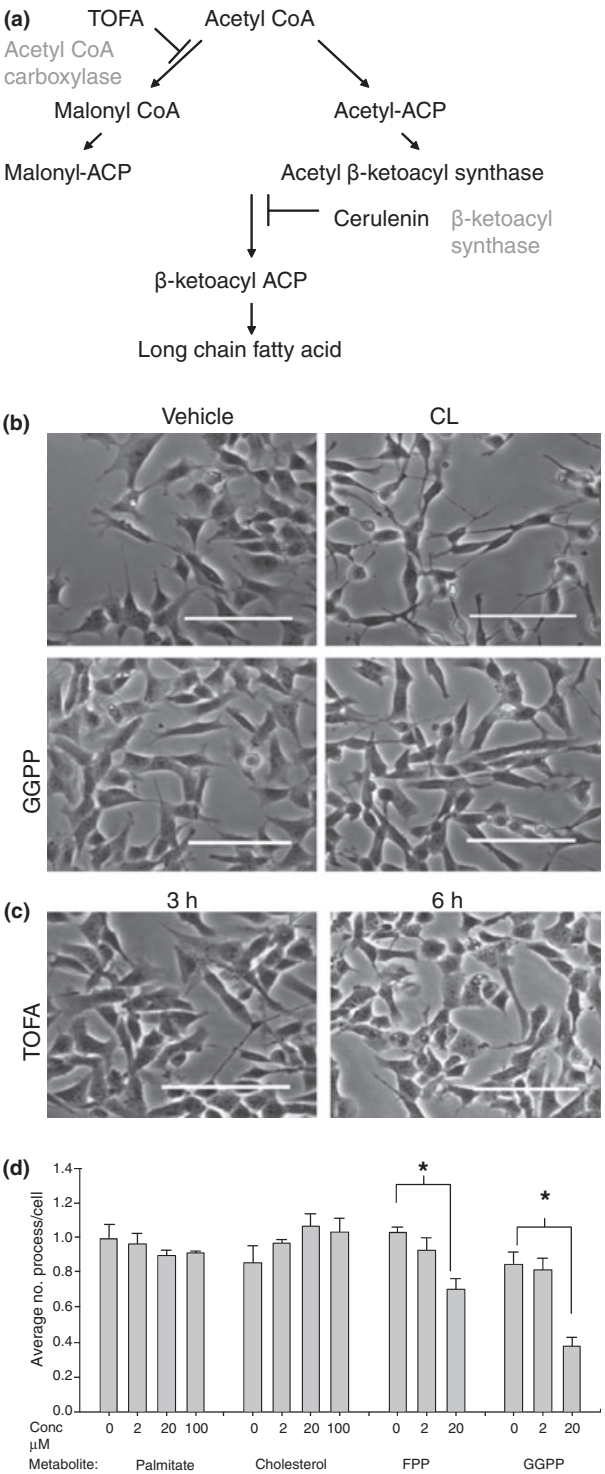

Fig. 3 Cerulenin (CL) induces a morphological change in SH-SY5Y by inhibiting isoprenoid synthesis. (a) Fatty acid synthetic pathway showing point of inhibition by tetradecyloxy-2 furoic acid (TOFA). (b) Swedish mutation amyloid precursor protein$_{K595N, M596L}$ (APP$_{swe}$) cells were treated with vehicle (top panel) or 20 μM geranylgeranyl pyrophosphate (GGPP; bottom panel) for 3 h prior to the addition of CL (100 μM) and incubation for a further 3 h. Scale bars represent 100 μm. (c) APP$_{swe}$ cells were treated with 10 μM TOFA for 3 or 6 h. (d) Relative number of processes observed in APP$_{swe}$ cells treated with increasing concentrations of palmitate, cholesterol, farnesyl pyrophosphate and GGPP. The numbers of processes are relative to the value for the vehicle control in each treatment. One-way ANOVA, $p < 0.05$, $n = 3$.

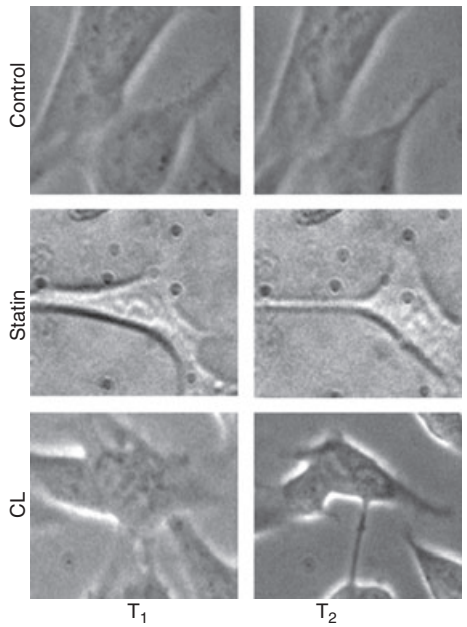

Fig. 4 Still images from video microscopy. Time interval between T_1 and T_2 is 24 min for each pair of images. Retraction of the cell body in Swedish mutation amyloid precursor protein$_{K595N, M596L}$ (APP$_{swe}$) cells to leave cell–cell (cerulenin, CL) or cell–substrate (Statin) contacts is clearly visible. No such retraction is detectable over the equivalent time frame in untreated APP$_{swe}$ cells. Control: Untreated APP$_{swe}$ cells. Statin: APP$_{swe}$ cells treated with10 μM Simvastatin. CL: APP$_{swe}$ cells treated with 100 μM CL.

referred to as 'tails' (Worthylake *et al.* 2001). Live-cell imaging of APP$_{swe}$ cells treated with CL revealed that the predominant event is cell contraction or rounding. As the cells round, contacts with the surface and between cells are maintained leaving long process. These were retracted later (Video S2). Over a similar time scale, after brief (4 h) treatment of APP$_{swe}$ cells with statin, the cells remain essential flat but some processes are generated by retraction of the cell body. (Fig. 4 and Video S3). The generation of processes by statin treatment is not complete until approximately 18 h after treatment. To investigate the dynamics of these processes at this time, live-cell imaging was carried out after 18 h of treatment. Initially cells were rounded, but spread before rounding again over a period of 150 min (Video S4). Importantly, the processes and some cell–cell contacts are maintained during this cycle of rounding and

spreading. The key finding from this set of experiments is that there is no evidence for positive outgrowth. Processes are generated through the stability of cell–cell and cell–surface contacts as the cells round up.

One anticipated consequence of the inhibition of isoprenoid biosynthesis by CL would be a reduction in fatty acid modification of the GTPase Rho. This would lead to reduced membrane association and inactivation of downstream effectors, such as the Rho-dependent kinase ROCK. Inhibition of this pathway leads to the generation of neurite-like processes and inhibits tail retraction which requires active Rho/ROCK (Worthylake *et al.* 2001; Fernandez-Hernando *et al.* 2005; Darenfed *et al.* 2007; Lingor *et al.* 2007). However, the data presented here indicates that outgrowth does not occur, indicating that CL does not act by this mechanism and that the Rho–ROCK pathway may still be functional in the presence of CL. To test this, APP_{swe} cells were treated with the ROCK inhibitor, Y27632 (Mueller *et al.* 2005). APP_{swe} cells pre-treated with Y27632 had a greater than average number of processes per cell but Y27632 had no effect on CL-induced cell rounding (Fig. 5a). In addition, cells treated with Y27632 showed processes which were more branched and often terminated with flat projections (Fig. 5b). Importantly, video microscopy revealed that in APP_{swe} cells co-treated with Y27632 and CL processes are still generated and new branches are formed from these processes (Fig. 5b and Video S5). These initial findings indicate that the Rho–ROCK signalling pathway is still active in the presence of CL and suggest that the effects of mevalonate inhibition are not mediated through the Rho–ROCK pathway.

Conclusions

The key conclusions from our data are that (i) the processes observed in cells in which mevalonate synthesis is blocked are not formed by positive outgrowth from the cell body, (ii) the dominant movement under these conditions is cell rounding, and (iii) processes are maintained whilst the cell rounds but may subsequently be retracted into the cell. On the basis of these observations, we suggest that the contradictory reports in the literature are likely a consequence of the different times at which static images are collected. We also conclude that the greater number of processes observed in APP_{swe} cells compared with $5Y^0$ cells treated with CL is the result of an increased persistence of processes in the APP over-expressing cells.

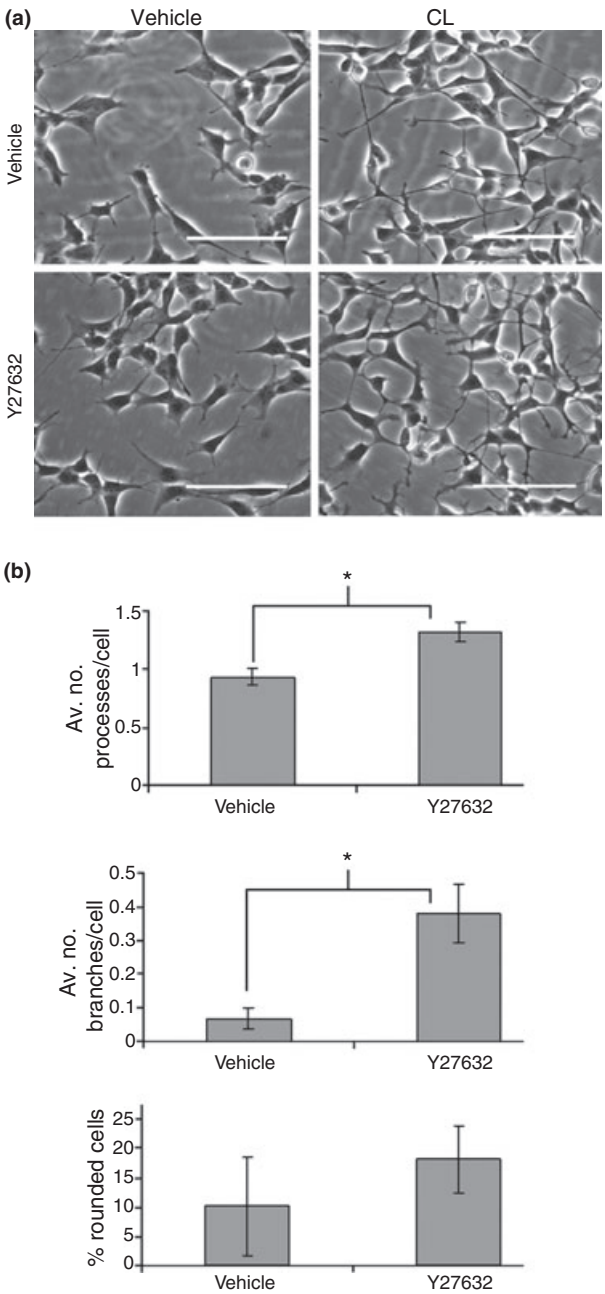

Fig. 5 ROCK inhibition with Y27632 indicates an active Rho/ROCK pathway is maintained in the presence of cerulenin (CL). (a) Swedish mutation amyloid precursor $protein_{K595N,\ M596L}$ (APP_{swe}) cells pre-treated with vehicle or Y27632 (10 μM) for 3 h (left panels) followed by 3 h further incubation (right panels) in the presence of CL (100 μM). Scale bars represent 100 μm. (b) The average number of processes, branches and % rounded cells observed in APP_{swe} cells treated with Y27632 (10 μM) for 3 h followed by 3 h further incubation in the presence of CL (100 μM). Student's *t*-test, $p < 0.05$, $n = 3$.

Discussion

Following the clinical findings that stain use is associated with a reduced risk of dementia, there has been considerable research aimed at unravelling the mechanistic basis of this effect. Despite this effort, no clear picture has emerged. For example, statins with similar chemical structures and of similar effectiveness in the inhibition of HMG-CoA reductase differ in their ability to cross the blood–brain barrier (Saheki *et al.* 1994). Hence, there is no simple correlation

between the ability of a given statin to cross the blood–brain barrier and reported benefit. There is general agreement, however that the statins impact on amyloidogenesis, but this appears to be independent of cholesterol lowering activity (Sjogren *et al.* 2003; Masse *et al.* 2005). This is consistent with a recent study which indicates that in the AD brain cholesterol homeostasis is unaffected but isoprenoid homeostasis is dysregulated (Eckert *et al.* 2009).

In addition to their effects on amyloidogenesis, the statins have been shown to affect neuronal morphology which could have a profound influence on function and survival. It has been shown for example that statins induce the formation of neurite-like structures (Maltese and Sheridan 1985; Fernandez-Hernando *et al.* 2005). As there are several contradictory reports in the literature, we have addressed this issue directly by undertaking a study of the dynamics of these morphological changes. Using video microscopy, we have been able to demonstrate clearly that blockade of the mevalonate pathway induces cell rounding and that these effects are isoprenoid rather than cholesterol dependent. Projections or neurite-like structures arise from the ability of points of contact between cells or with the surface to persist while the cell body retracts rather than through a process of extension or outgrowth. These changes are rapid and cyclical making it possible to observe quite different morphologies during a given time frame. Therefore, our key finding is that mevalonate blockade does not promote neurite outgrowth, which in some reports has been interpreted as the basis of the beneficial effects of the statins in AD (Pooler *et al.* 2006). Previous observations of distinct cellular structures or morphologies using conventional microscopy are effectively snapshots and the observed result depends critically on timing.

Simvastatin and CL block mevalonate biosynthesis at sequential steps in the pathway. Both elicited the same type of change in cells but we observed distinct differences. First, we found a significant difference in the time taken for the morphological changes to develop, with CL producing an effect much more rapidly. This difference may arise from the differing pharmacology of the inhibitors. Simvastatin is a reversible inhibitor whereas CL is an irreversible inhibitor, certainly for β ketoacyl synthase where it forms a covalent bond with the active site cysteine (Funabashi *et al.* 1989; Price *et al.* 2001). The similar active site chemistry suggests that CL is likely to inhibit HMG-CoA synthase through a similar mechanism (Haapalainen *et al.* 2006). Second, CL treatment produced different results in non-transfected SH-SY5Y cells compared with cells over-expressing APP while Simvastatin did not. Process generation was rapidly and clearly evident only in the APP expressing cells treated with CL, while simvastatin produced the same response in both cell lines. This suggests that CL may inhibit an additional pathway which impacts on cell rounding. However, we have tested the role of palmitate and other lipids and specifically blocked acetylCo-A carboxylase and the results indicate a specific role for the isoprenoid GGPP in the CL-mediated effect. We were also able to establish that the Rho/ROCK pathway is still active when cells are treated with CL. Clearly further analysis of the pharmacology of CL is required but the results highlight an important cell adhesion related role for APP.

The role of APP in cell adhesion in both the peripheral and CNS has been studied in great detail (Reinhard *et al.* 2005). Despite this, there have been few studies of the direct effects of APP expression on neuronal morphology. Most transgenic mouse models in which a mutant form of human APP is over-expressed have focussed on damage to dendrites linked to the accumulation of Aβ. However, it has been shown in young APP knockout animals that dendritic spines are reduced in length (Seabrook *et al.* 1999), while they are longer in APP over-expressing animals (Rocher *et al.* 2008) suggesting that APP may play a direct role in aspects of neuronal morphology. Cell culture and structural studies support the view that trans-dimerisation of APP promotes cell–cell adhesion (Soba *et al.* 2005; Kaden *et al.* 2008). Recently, the use of conditional knockout mice with tissue-specific deletion of APP revealed that pre-synaptic and post-synaptic APP act in concert to mediate neuromuscular synapse assembly (Wang *et al.* 2009). This is considered to also underlie APP function in CNS synapses (Wang *et al.* 2009). Using a mixed culture assay containing HEK293 cells over-expressing human APP and mouse primary neurons it was possible to observe formation of synaptic puncta which was dependent on the expression of full-length APP at the cell surface of the non-neuronal cell line (Wang *et al.* 2009). This pivotal study shows that APP over-expression systems can provide crucial information in the evaluation of the contribution of APP to cell adhesion and is consistent with our observation that SH-SY5Y cells over-expressing APP are able to form stable cell–cell and cell–surface contacts. We have also established that such contacts remain stable in the context of significant changes in cell morphology induced by mevalonate pathway blockade.

Acknowledgement

We would like to thank Dr Joerg W. Bartsch and Dr David Howlett for comments on the manuscript.

Supporting information

Additional Supporting Information may be found in the online version of this article:

Figure S1. The number of processes generated by 5Y0 and APPswe is dependent on seeding density.

Figure S2. APPswe cells show increased adherence to tissue culture plastic compared to 5Y0.

Figure S3. RT-PCR shows no increase in the expression of markers of differentiation in APPswe cells when treated with CL.

Table S1. Average number of processes observed per cell in APPswe cells under the conditions indicated.

Video S1. Control. UntreatedAPPswe cells.

Video S2. APPswe cells treated with 100μM CL.

Video S3. APPswe cells treated with10 μM Simvastatin.

Video S4. APPswe following 18 h treated with Simvastatin.

Video S5. APPswe cells incubated with Y27632 then treated with CL Cells round up leaving clear protrusions attached to the surface.

As a service to our authors and readers, this journal provides supporting information supplied by the authors. Such materials are peer-reviewed and may be re-organized for online delivery, but are not copy-edited or typeset. Technical support issues arising from supporting information (other than missing files) should be addressed to the authors.

References

Agarwal B., Halmos B., Feoktistov A. S., Protiva P., Ramey W. G., Chen M., Pothoulakis C., Lamont J. T. and Holt P. R. (2002) Mechanism of lovastatin-induced apoptosis in intestinal epithelial cells. *Carcinogenesis* **23**, 521–528.

Alberts A. W. (1990) Lovastatin and simvastatin – inhibitors of HMG CoA reductase and cholesterol biosynthesis. *Cardiology* **77** (Suppl. 4), 14–21.

Araki W., Kitaguchi N., Tokushima Y., Ishii K., Aratake H., Shimohama S., Nakamura S. and Kimura J. (1991) Trophic effect of beta-amyloid precursor protein on cerebral cortical neurons in culture. *Biochem. Biophys. Res. Commun.* **181**, 265–271.

Brown M. S. and Goldstein J. L. (2009) Cholesterol feedback: from Schoenheimer's bottle to Scap's MELADL. *J. Lipid Res.* **50**(Suppl.), S15–S27.

Chung K. S., Sun N. K., Lee S. H. *et al.* (2006) Cerulenin-mediated apoptosis is involved in adenine metabolic pathway. *Biochem. Biophys. Res. Commun.* **349**, 1025–1031.

Clarris H. J., Nurcombe V., Small D. H., Beyreuther K. and Masters C. L. (1994) Secretion of nerve growth factor from septum stimulates neurite outgrowth and release of the amyloid protein precursor of Alzheimer's disease from hippocampal explants. *J. Neurosci. Res.* **38**, 248–258.

Cole S. L. and Vassar R. (2006) Isoprenoids and Alzheimer's disease: a complex relationship. *Neurobiol. Dis.* **22**, 209–222.

Constantinescu R., Constantinescu A. T., Reichman H. and Janetzky B. (2007) Neuronal differentiation and long-term culture of the human neuroblastoma line SH-SY5Y. *J. Neural. Transm.* **Suppl 72**, 17–28.

Cordy J. M., Hussain I., Dingwall C., Hooper N. M. and Turner A. J. (2003) Exclusively targeting beta-secretase to lipid rafts by GPI-anchor addition up-regulates beta-site processing of the amyloid precursor protein. *Proc. Natl Acad. Sci. USA* **100**, 11735–11740.

Darenfed H., Dayanandan B., Zhang T., Hsieh S. H., Fournier A. E. and Mandato C. A. (2007) Molecular characterization of the effects of Y-27632. *Cell Motil. Cytoskeleton* **64**, 97–109.

Eckert G. P., Hooff G. P., Strandjord D. M., Igbavboa U., Volmer D. A., Muller W. E. and Wood W. G. (2009) Regulation of the brain isoprenoids farnesyl- and geranylgeranylpyrophosphate is altered in male Alzheimer patients. *Neurobiol. Dis.* **35**, 251–257.

Ehehalt R., Keller P., Haass C., Thiele C. and Simons K. (2003) Amyloidogenic processing of the Alzheimer beta-amyloid precursor protein depends on lipid rafts. *J. Cell Biol.* **160**, 113–123.

Fassbender K., Simons M., Bergmann C. *et al.* (2001) Simvastatin strongly reduces levels of Alzheimer's disease beta -amyloid peptides Abeta 42 and Abeta 40 in vitro and in vivo. *Proc. Natl Acad. Sci. USA* **98**, 5856–5861.

Fernandez-Hernando C., Suarez Y. and Lasuncion M. A. (2005) Lovastatin-induced PC-12 cell differentiation is associated with RhoA/RhoA kinase pathway inactivation. *Mol. Cell. Neurosci.* **29**, 591–602.

Fonseca A. C., Resende R., Oliveira C. R. and Pereira C. M. (2009) Cholesterol and statins in Alzheimer's disease: current controversies. *Exp. Neurol.* **223**, 282–293.

Funabashi H., Kawaguchi A., Tomoda H., Omura S., Okuda S. and Iwasaki S. (1989) Binding site of cerulenin in fatty acid synthetase. *J. Biochem.* **105**, 751–755.

Guarnieri S., Pilla R., Morabito C., Sacchetti S., Mancinelli R., Fano G. and Mariggio M. A. (2009) Extracellular guanosine and GTP promote expression of differentiation markers and induce S-phase cell-cycle arrest in human SH-SY5Y neuroblastoma cells. *Int. J. Dev. Neurosci.* **27**, 135–47.

Golde T. E. and Younkin S. G. (2001) Presenilins as therapeutic targets for the treatment of Alzheimer's disease. *Trends Mol. Med.* **7**, 264–269.

Haapalainen A. M., Merilainen G. and Wierenga R. K. (2006) The thiolase superfamily: condensing enzymes with diverse reaction specificities. *Trends Biochem. Sci.* **31**, 64–71.

Hoglund K. and Blennow K. (2007) Effect of HMG-CoA reductase inhibitors on beta-amyloid peptide levels: implications for Alzheimer's disease. *CNS Drugs* **21**, 449–462.

Hussain I., Hawkins J., Harrison D. *et al.* (2007) Oral administration of a potent and selective non-peptidic BACE-1 inhibitor decreases beta-cleavage of amyloid precursor protein and amyloid-beta production in vivo. *J. Neurochem.* **100**, 802–809.

Itoh N., Okochi M., Tagami S. *et al.* (2009) Destruxin E Decreases Beta-Amyloid Generation by Reducing Colocalization of Beta-Amyloid-Cleaving Enzyme 1 and Beta-Amyloid Protein Precursor. *Neurodegener. Dis.* **6**, 230–239.

Jick H., Zornberg G. L., Jick S. S., Seshadri S. and Drachman D. A. (2000) Statins and the risk of dementia. *Lancet* **356**, 1627–1631.

Jin L. W., Ninomiya H., Roch J. M., Schubert D., Masliah E., Otero D. A. and Saitoh T. (1994) Peptides containing the RERMS sequence of amyloid beta/A4 protein precursor bind cell surface and promote neurite extension. *J. Neurosci.* **14**, 5461–5470.

Kaden D., Munter L. M., Joshi M. *et al.* (2008) Homophilic Interactions of the Amyloid Precursor Protein (APP) Ectodomain Are Regulated by the Loop Region and Affect +|-Secretase Cleavage of APP. *J. Biol. Chem.* **283**, 7271–7279.

Kim W. Y., Gonsiorek E. A., Barnhart C. *et al.* (2009) Statins decrease dendritic arborization in rat sympathetic neurons by blocking RhoA activation. *J. Neurochem.* **108**, 1057–1071.

Kinoshita A., Fukumoto H., Shah T., Whelan C. M., Irizarry M. C. and Hyman B. T. (2003) Demonstration by FRET of BACE interaction with the amyloid precursor protein at the cell surface and in early endosomes. *J. Cell Sci.* **116**, 3339–3346.

Koch G., Benz C., Schmidt G., Olenik C. and Aktories K. (1997) Role of Rho protein in lovastatin-induced breakdown of actin cytoskeleton. *J. Pharmacol. Exp. Ther.* **283**, 901–909.

Kojro E., Gimpl G., Lammich S., Marz W. and Fahrenholz F. (2001) Low cholesterol stimulates the nonamyloidogenic pathway by its effect on the alpha -secretase ADAM 10. *Proc. Natl Acad. Sci. USA* **98**, 5815–5820.

Kroschewski R., Hall A. and Mellman I. (1999) Cdc42 controls secretory and endocytic transport to the basolateral plasma membrane of MDCK cells. *Nat. Cell Biol.* **1**, 8–13.

Lingor P., Teusch N., Schwarz K., Mueller R., Mack H., Bahr M. and Mueller B. K. (2007) Inhibition of Rho kinase (ROCK) increases neurite outgrowth on chondroitin sulphate proteoglycan in vitro

and axonal regeneration in the adult optic nerve in vivo. *J. Neurochem.* **103**, 181–189.

Maillet M., Robert S. J., Cacquevel M., Gastineau M., Vivien D., Bertoglio J., Zugaza J. L., Fischmeister R. and Lezoualc'h F. (2003) Crosstalk between Rap1 and Rac regulates secretion of sAPPalpha. *Nat. Cell Biol.* **5**, 633–639.

Maltese W. A. and Sheridan K. M. (1985) Differentiation of neuroblastoma cells induced by an inhibitor of mevalonate synthesis: relation of neurite outgrowth and acetylcholinesterase activity to changes in cell proliferation and blocked isoprenoid synthesis. *J. Cell. Physiol.* **125**, 540–558.

Malvoisin E. and Wild F. (1990) Effect of drugs which inhibit cholesterol synthesis on syncytia formation in vero cells infected with measles virus. *Biochim. Biophys. Acta* **1042**, 359–364.

Masse I., Bordet R., Deplanque D., Al Khedr A., Richard F., Libersa C. and Pasquier F. (2005) Lipid lowering agents are associated with a slower cognitive decline in Alzheimer's disease. *J. Neurol. Neurosurg. Psychiatry* **76**, 1624–1629.

McConlogue L., Castellano F., deWit C., Schenk D. and Maltese W. A. (1996) Differential effects of a Rab6 mutant on secretory versus amyloidogenic processing of Alzheimer's beta-amyloid precursor protein. *J. Biol. Chem.* **271**, 1343–1348.

Meske V., Albert F., Richter D., Schwarze J. and Ohm T. G. (2003) Blockade of HMG-CoA reductase activity causes changes in microtubule-stabilizing protein tau via suppression of geranylgeranylpyrophosphate formation: implications for Alzheimer's disease. *Eur. J. Neurosci.* **17**, 93–102.

Monaghan T. K., MacKenzie C. J., Plevin R. and Lutz E. M. (2007) PACAP-38 induces neuronal differentiation of human SH-SY5Y neuroblastoma cells via cAMP-mediated activation of ERK and p38 MAP kinases. *J. Neurochem.* **104**, 74–88.

Morohashi Y., Kan T., Tominari Y. *et al.* (2006) C-terminal fragment of presenilin is the molecular target of a dipeptidic gamma-secretase-specific inhibitor DAPT (N-[N-(3,5-difluorophenacetyl)-L-alanyl]-S-phenylglycine t-butyl ester). *J. Biol. Chem.* **281**, 14670–14676.

Moss M. L., Bomar M., Liu Q. *et al.* (2007) The ADAM10 prodomain is a specific inhibitor of ADAM10 proteolytic activity and inhibits cellular shedding events. *J. Biol. Chem.* **282**, 35712–35721.

Mueller B. K., Mack H. and Teusch N. (2005) Rho kinase, a promising drug target for neurological disorders. *Nat. Rev. Drug Discov.* **4**, 387–398.

Ohsawa I., Hirose Y., Ishiguro M., Imai Y., Ishiura S. and Kohsaka S. (1995) Expression, purification, and neurotrophic activity of amyloid precursor protein-secreted forms produced by yeast. *Biochem. Biophys. Res. Commun.* **213**, 52–58.

Omura S. (1976) The antibiotic cerulenin, a novel tool for biochemistry as an inhibitor of fatty acid synthesis. *Bacteriol. Rev.* **40**, 681–697.

Ostrowski S. M., Wilkinson B. L., Golde T. E. and Landreth G. (2007) Statins reduce amyloid-beta production through inhibition of protein isoprenylation. *J. Biol. Chem.* **282**, 26832–26844.

Parsons R. B., Subramaniam D. and Austen B. M. (2007) A specific inhibitor of cholesterol biosynthesis, BM15.766, reduces the expression of beta-secretase and the production of amyloid-beta in vitro. *J. Neurochem.* **102**, 1276–1291.

Pedrini S., Carter T. L., Prendergast G., Petanceska S., Ehrlich M. E. and Gandy S. (2005) Modulation of statin-activated shedding of Alzheimer APP ectodomain by ROCK. *PLoS Med.* **2**, e18.

Pimenta A. S., Gaidhu M. P., Habib S., So M., Fediuc S., Mirpourian M., Musheev M., Curi R. and Ceddia R. B. (2008) Prolonged exposure to palmitate impairs fatty acid oxidation despite activation of AMP-activated protein kinase in skeletal muscle cells. *J. Cell. Physiol.* **217**, 478–485.

Pizer E. S., Thupari J., Han W. F., Pinn M. L., Chrest F. J., Frehywot G. L., Townsend C. A. and Kuhajda F. P. (2000) Malonyl-coenzyme-A is a potential mediator of cytotoxicity induced by fatty-acid synthase inhibition in human breast cancer cells and xenografts. *Cancer Res.* **60**, 213–218.

Pooler A. M., Xi S. C. and Wurtman R. J. (2006) The 3-hydroxy-3-methylglutaryl co-enzyme A reductase inhibitor pravastatin enhances neurite outgrowth in hippocampal neurons. *J. Neurochem.* **97**, 716–723.

Price A. C., Choi K. H., Heath R. J., Li Z., White S. W. and Rock C. O. (2001) Inhibition of beta-ketoacyl-acyl carrier protein synthases by thiolactomycin and cerulenin. Structure and mechanism. *J. Biol. Chem.* **276**, 6551–6559.

Qiu W. Q., Ferreira A., Miller C., Koo E. H. and Selkoe D. J. (1995) Cell–surface beta-amyloid precursor protein stimulates neurite outgrowth of hippocampal neurons in an isoform-dependent manner. *J. Neurosci.* **15**, 2157–2167.

Rajendran L., Honsho M., Zahn T. R., Keller P., Geiger K. D., Verkade P. and Simons K. (2006) Alzheimer's disease beta-amyloid peptides are released in association with exosomes. *Proc. Natl Acad. Sci. USA* **103**, 11172–11177.

Reinhard C., Hebert S. S. and De Strooper B. (2005) The amyloid-β precursor protein: integrating structure with biological function. *EMBO J.* **24**, 3996–4006.

Resh M. D. (2006) Trafficking and signaling by fatty-acylated and prenylated proteins. *Nat. Chem. Biol.* **2**, 584–590.

Riddell D. R., Christie G., Hussain I. and Dingwall C. (2001) Compartmentalization of beta-secretase (Asp2) into low-buoyant density, noncaveolar lipid rafts. *Curr. Biol.* **11**, 1288–1293.

Rocher A. B., Kinson M. S. and Luebke J. I. (2008) Significant structural but not physiological changes in cortical neurons of 12-month-old Tg2576 mice. *Neurobiol. Dis.* **32**, 309–318.

Saheki A., Terasaki T., Tamai I. and Tsuji A. (1994) In vivo and in vitro blood-brain barrier transport of 3-hydroxy-3-methylglutaryl coenzyme A (HMG-CoA) reductase inhibitors. *Pharm. Res.* **11**, 305–311.

Schmidt R. A., Glomset J. A., Wight T. N., Habenicht A. J. and Ross R. (1982) A study of the Influence of mevalonic acid and its metabolites on the morphology of swiss 3T3 cells. *J. Cell Biol.* **95**, 144–153.

Schulz J. G., Bosel J., Stoeckel M., Megow D., Dirnagl U. and Endres M. (2004) HMG-CoA reductase inhibition causes neurite loss by interfering with geranylgeranylpyrophosphate synthesis. *J. Neurochem.* **89**, 24–32.

Seabrook G. R., Smith D. W., Bowery B. J. *et al.* (1999) Mechanisms contributing to the deficits in hippocampal synaptic plasticity in mice lacking amyloid precursor protein. *Neuropharmacology* **38**, 349–359.

Simons M., Keller P., De S. B., Beyreuther K., Dotti C. G. and Simons K. (1998) Cholesterol depletion inhibits the generation of beta-amyloid in hippocampal neurons. *Proc. Natl Acad. Sci. USA* **95**, 6460–6464.

Simpson P. B., Bacha J. I., Palfreyman E. L., Woollacott A. J., McKernan R. M. and Kerby J. (2001) Retinoic acid-evoked differentiation of neuroblastoma cells predominates over growth-factor stimulation: an automated image capture and quantitation approach to neuritogenesis. *Analyt. Biochem.* **298**, 163–169.

Sisodia S. S. (1992) Beta-amyloid precursor protein cleavage by a membrane-bound protease. *Proc. Natl Acad. Sci. USA* **89**, 6075–6079.

Sjogren M., Gustafsson K., Syversen S., Olsson A., Edman A., Davidsson P., Wallin A. and Blennow K. (2003) Treatment with simvastatin in patients with Alzheimer's disease lowers both α and ß-cleaved amyloid precursor protein. *Dementia Geriatr. Cogn. Disord.* **16**, 25–30.

Small S. A. and Gandy S. (2006) Sorting through the cell biology of Alzheimer's disease: intracellular pathways to pathogenesis. *Neuron* **52**, 15–31.

Soba P., Eggert S., Wagner K. *et al.* (2005) Homo- and heterodimerization of APP family members promotes intercellular adhesion. *EMBO J.* **24**, 3624–3634.

Walsh D. M., Tseng B. P., Rydel R. E., Podlisny M. B. and Selkoe D. J. (2000) The oligomerization of amyloid beta-protein begins intracellularly in cells derived from human brain. *Biochemistry* **39**, 10831–10839.

Wang Z., Wang B., Yang L., Guo Q., Aithmitti N., Songyang Z. and Zheng H. (2009) Presynaptic and postsynaptic interaction of the amyloid precursor protein promotes peripheral and central synaptogenesis. *J. Neurosci.* **29**, 10788–10801.

Wolozin B., Kellman W., Ruosseau P., Celesia G. G. and Siegel G. (2000) Decreased prevalence of Alzheimer disease associated with 3-hydroxy-3-methyglutaryl coenzyme A reductase inhibitors. *Arch. Neurol.* **57**, 1439–1443.

Won J. S., Im Y. B., Khan M., Contreras M., Singh A. K. and Singh I. (2008) Lovastatin inhibits amyloid precursor protein (APP) beta-cleavage through reduction of APP distribution in Lubrol WX extractable low density lipid rafts. *J. Neurochem.* **105**, 1536–1549.

Worthylake R. A., Lemoine S., Watson J. M. and Burridge K. (2001) RhoA is required for monocyte tail retraction during transendothelial migration. *J. Cell Biol.* **154**, 147–160.

Zamrini E., McGwin G. and Roseman J. M. (2004) Association between statin use and Alzheimer's disease. *Neuroepidemiology* **23**, 94–98.

